REMOTE SENSING IMAGE-BASED ANALYSIS OF THE RELATIONSHIP BETWEEN URBAN HEAT ISLAND AND VEGETATION FRACTION

Liqin Cao, Pingxiang Li, Liangpei Zhang, Tao Chen

State Key Laboratory of information Engineering in Surveying, Mapping and Remote Sensing(LIESMARS), Wuhan University，129 Luoyu Road, Wuhan, 430079 ,China- Caoliqin0823@126.com

Commission VII, ICWG-VII-IV

ABSTRACT:

As the relationship between land surface temperature (LST) and Normalized Difference Vegetation Index (NDVI) can not be able to effectively apply after NDVI reached saturation[1]. In this study, the vegetation fraction, which derived from Dimidiate Pixel Model, as the indicator of vegetation abundance has been introduced to analyze remote sensing of the change of urban heat islands (UHIs). Landsat TM and ETM+ images of Wuhan from 1988 to 2002 were selected to retrieve the brightness temperatures and vegetation fraction. Results show that, from 1988 to 2002, the intensity of UHI was increased and the average vegetation fraction of the whole region was decreased. The urban ratio index (URI) of the study area was increased from 0.153 to 0.170 and the average vegetation fraction decreased from 58.41% to 50.45%. Our analysis showed that the UHI effect has become more prominent in areas of rapid changes as its vegetation fraction decreasing in the past decade. The brightness temperature had strong correlation with vegetation fraction，and the coefficient of determination value (R^2) was 0.867, 0.843, 0.841, 0.843 of 1988, 1991, 1996 and 2002.

1. INTRODUCTION

Urban heat island (UHI) has long been a concern for more than 40 years. UHI studies have traditionally been conducted for isolated locations and with in situ measurements of air temperatures. The advent of satellite remote sensing technology has made it possible to study UHI both remotely and on continental or global scale. Studies on the UHI phenomenon using satellite derived land surface temperature (LST) measurements have been conducted using various remote sending data such as NOAA AVHRR with 1.1km spatial resolutions[2~7], Landsat Thermatic Mapper (TM) and Enhanced Therntic Mapper Plus (ETM+) thermal infrared (TIR) data with 120m and 60m spatial resolutions, respectively, and so on. Researches on LST show that the partition of sensible and latent heat fluxes and thus surface radiant temperature response is a function of varying surface soil water content and vegetation cover. A higher level of latent heat exchange was found with more vegetated areas, while sensible heat exchange was more favored by sparsely vegetated such as urban areas. This finding encourages more and more research focusing on the relationship between LST and vegetation abundance[8~11]. Remote sensing of UHI has traditionally used the NDVI as the indicator of vegetation abundance to estimate the LST-vegetation relationship[1]. However, LST-NDVI feature space will not be able to effectively apply when NDVI reached saturation. Vegetation fraction is an important index to scale the status of the vegetation of the region, and frequently used in monitoring vegetation status and the exchange of energy. In this study, using a Landsat TM and ETM+ imagery of the city of Wuhan, our purpose is to investigate the impact of the vegetation fraction changes on the intensity of the UHI effect in the region. Specific objectives of this research are: (1) to derived brightness temperature from Landsat TM/ETM+ thermal band for the period 1988-2002; (2) to estimate vegetation fraction for different times; (3) to investigate the change of brightness temperature and vegetation fraction in the city of Wuhan for 14 years; and (4) to quantitatively and quantitatively study the relationship between the intensity of UHI and vegetation fraction and how it has changed over time.

2. DATA AND METHODS

2.1 Study Area

The City of Wuhan, located in Hubei Province, has been chosen as the area of study. The city is located on a flat plain, located between 113°41'E~115°05'E and 29°50'N ~31°22'N, with the area of 8467.6km2. The study areas include the center urban of the city and three suburbs (Caidian, Hannan and Jiangxia)(Fig1). Huangpi and Xinzhou are excluded because of limitations of data. Detecting the relationship between UHI development and vegetation fraction is significant to understand, control, and plan the city's future development.
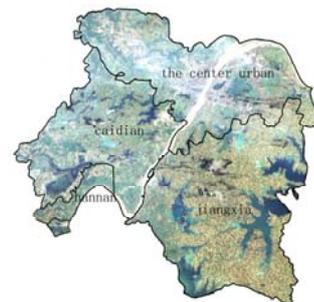

Figure 1. the false image of the study area

2.2 Image pre-processing

Landsat 7 Enhanced Thematic Mapper Plus (ETM+) image (Oct 13, 2002) and Landsat 5 TM images (Oct 26, 1988; Oct 23, 1991; Oct 4, 1996) were used in this research. The data acquisition date has a highly clear atmospheric condition. All images bands 1-5 and 7 have a spatial resolution of 30m, and the thermal infrared band (band6) has a spatial resolution of 120m for Landsat 5 TM images and 60m for Landsat 7 ETM+ images. The Landsat image were further rectified to a common Universal Transverse Mercator coordinate system based on 1:24,000 scale topographic maps, and were resampled using the nearest neighbor algorithm with a pixel size of 30 by 30 m for all bands including the thermal band. The resultant RMSE was found to be less than 0.5 pixels.

2.3 Derivation of LST from Landsat TM/ETM+ imagery

The LST were derived from the corrected TM/ETM+ TIR band. The local time of satellite overpasses was in the morning (approximately 11:00 AM) (this was the best image available), so that the chance for detecting a weaken UHI is maximized. The following equation was used to convert the digital number (DN) of Landsat TM/ETM+ TIR band into spectral radiance[12].For Landst-5 TM, Chen at al proposed a method of deriving brightness temperature. First, the digital numbers (DNs) of band6 are converted to radiation luminance (R_{TM6}, $mW * cm^{-2} * sr^{-1}$) by the following formula:

$$R_{TM6} = 0.0068337 \times DN + 0.1534 \qquad (1)$$

The next step is to convert the radiance luminance to at-satellite brightness temperature (i.e., blackbody temperature, TB) under the assumption of uniform emissivity. The conversion formula is:

$$T_B = \frac{K_1}{\ln(\dfrac{K_2}{R_{TM6}/b} + 1)} \qquad (2)$$

where TB is effective at-satellite temperature in K; K_1 and K_2 are pre-launch calibration constants. $K_1 = 1260.56K$,

and $K_2 = 60.766 (mW * cm^{-2} * sr^{-1} * \mu m^{-1})$, b represents effective spectral range, when the sensor's response is much more than 50%, $b = 1.239(\mu m)$.

For Landsat-7 ETM+, it is also simplified to two separate steps. First, the DNs of band6 were converted to radiance by the following formula:

$Radiance = gain * DN + offset$; Then the effective at-satellite temperature of the viewed Earth-atmosphere system under the assumption of a uniform emissivity could be obtained from the above spectral radiance by the following equation:

$$T_B = \frac{K_1}{\ln(K_2 / L_\lambda + 1)} \qquad (3)$$

Where, $K_1 = 1282.71K$ and $K_2 = 666.09(mW * cm^{-2} * sr^{-1} * \mu m^{-1})$ are calibration constants; and L_λ is the spectral radiance in $mW * cm^{-2} * sr^{-1} * \mu m^{-1}$.

2.4 Estimation of vegetation fraction using Dimidiate Pixel Model

Dimidiate Pixel Model [13~15] assumes that a pixel consists of two components: pure vegetation and non-vegetation, so the reflectance of any pixel can be presented as follows:

$$R = R_v + R_s \qquad (4)$$

Where R_v is the reflectance of pure vegetation while R_s is the reflectance of non-vegetation.

We assume that the vegetation coverage proportion of a pixel is fc, that is the vegetation fraction, then the non-vegetation coverage proportion of the pixel is $1 - fc$. If the whole pixel is covered by vegetation, the reflectance we gain is R_{veg}; if it has no vegetation coverage, the reflectance is R_{soil}, so R_v and R_s of a mixed pixel can be presented as a product of R_{veg} and fc (Eq(5)), R_{soil} and $1 - fc$ (Eq(6)), respectively:

$$R_v = fc * R_{veg} \qquad (5)$$
$$R_s = (1\text{-}fc) * R_{soil} \qquad (6)$$

Through computing Eq (4), Eq (5) and Eq (6) together, we acquire the equation of calculating vegetation fraction as follows:

$$fc = (R\text{-}R_{soil})/(R_{veg} - R_{soil}) \qquad (7)$$

Where R_{soil} and R_{vegl} are two key parameters of dimidiate pixel model. Obviously, if we get these two parameters, we can compute the vegetation fraction by using remote sensing information through eq (7).

$NDVI$ is the indication factor of vegetation growth state and the vegetation. According to dimidiate pixel model, we can express the $NDVI$ of each pixel as equation (8):

$$fc = \frac{NDVI - NDVI_{soil}}{NDVI_{veg} - NDVI_{soil}}$$

(8)

Where, $NDVI_{veg}$ is the $NDVI$ of a pure vegetation pixel while $NDVI_{soil}$ is the $NDVI$ of a pure soil pixel.

In theory, $NDVI_{soil}$ should be zero for most soil types, but it changes from -0.1 to 0.2[11,12] because of the influences of many factors. $NDVI_{veg}$ should be the maximum of $NDVI$, but it will change with the spatial or temporal change because of the influences of vegetation types. Thus, $NDVI_{veg}$ and $NDVI_{soil}$ can not be fixed values [13] even in the same image. Vegetation type changes with the change of the land use type. To the same land use type, vegetation types are same approximately [14], so the pixels' $NDVI_{veg}$ are close to the same vegetation type; the pixels' $NDVI_{soil}$ are close to the same soil type too. Thus, the land use map and the soil map may be used to compute $NDVI_{veg}$ and $NDVI_{soil}$.

3. RESULTS AND DISCUSSION

3.1 Characteristic of LST and temperature variation

The brightness temperature of Wuhan from 1988 to 2002 could be derived using formula (2) and (3). In order to minimize the impact of the time difference, the temperature was normalized to 0~1. Fig.2 shows the distribution of temperature
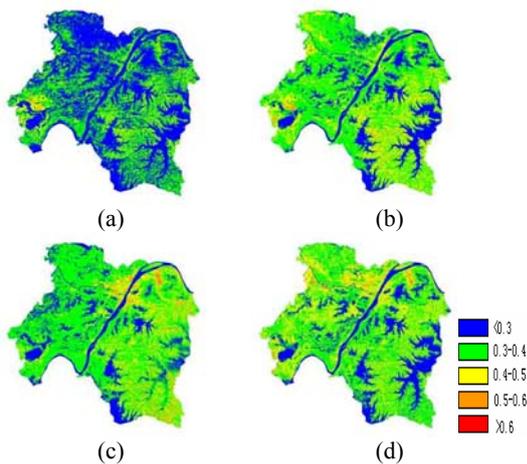

(a)   (b)

(c)   (d)

Figure.2 The normalized temperature distribution in the study area onOct 26, 1988(a), Oct 23, 1991(b), Oct 4, 1996(c) and Oct 13, 2002(d)

maps，from which we can see that the UHI had an increase trend in the process of fluctuations for the past 14 years, especially in the center urban. From 1996, the land surface temperature of the urban, n which there is industrial areas, new urban and densely populated residential areas, as much higher than that of the suburb, and the area of high land surface

temperature can be seemed as island and be easily recognized. Meanwhile, there was not a clear center of UHI in the center of the urban. There structure of UHI was complex inlaying and showed a pattern of distribution centers.

Table 1 represents the mean brightness of temperature of Caidian, Hanna, Jiangxia, the center urban and the whole region and the URI of the whole region for 14 years. It was found that the mean brightness of temperature of the whole region was increased from 13.37℃ to 22.98℃. As the development of urbanization, the quality of hot environment of the center urban also degraded seriously. The mean brightness temperature was increased in the study districts, especially in the center urban. Comparison between the mean temperature of Oct 26, 1988 and Oct 13, 2002 in the center urban shows that the values increased 9.12 ℃.

To analysis the change of UHI, Urban Heat Index (URI) was introduced, which was based on the ratio of UHI area to urban area. The greater the index is, the more intense of the UHI is. The trend of UHI showed a obvious trend: as the urban area expanded, the URI of Wuhan consistent increased, especially in 1991. The URI from 1988 to 2002 were 0.134, 0.153and 0.170, respectively.

3.2 Characteristic of Vegetation Fraction and its variation

	the mean brightness of temperature(℃)			
	1988	1991	1996	2002
Caidian	13.69	17.62	21.23	22.42
Hannan	13.19	17.31	21.33	23.16
Jiangxia	13.75	17.96	21.96	23.08
center urban	14.14	18.06	22.06	23.26
whole region	13.37	17.52	21.64	22.98
URI of whole region	0.134	0.153	0.158	0.170

Table 1 the mean brightness of temperature of different district and the URI of the whole region

This paper estimates vegetation fraction of Wuhan based on the $NDVI$ method for dimidiate pixel model. First, $NDVI$ of it is computed; then, the land use map and the soil map of the study area were used as reference to make a statistic of the whole $NDVI$ value. According to the frequency statistical table, the $NDVI$ frequency of 5% in the soil map was used as $NDVI_{soil}$, and that of 95% in the land use map was used as $NDVI_{veg}$; at last, $NDVI_{soil}$ and $NDVI_{veg}$ which obtained above were taken into equation (9). So we acquired the vegetation fraction map of the study area.

From the Fig 3, we can see that vegetation fraction in the center urban, where performed as the center, was lower than that in suburb. During the 14years, the vegetation fraction was highest in 1988 and lowest in 2002.

Table 2 shows the change of vegetation fraction in the multi-temporal. From 1988 to 1991, the average vegetation fraction of the whole region has dropped, but the overall downward trend is not very clear, only dropped 2.2%. The vegetation fraction in the center urban decreased significantly,

except the Dongxi Lakes. From 1991 to 1996 the vegetation fraction was lightly increased in the whole study area, rose 1.6%. From 1996 to 2002 is the period which vegetation fraction decreased the most sharply in this period, dropped 7.4%.The average vegetation fraction of the whole area from 1988 to 2002 was decreased from 58.41% to 50.45%, especially in Jiangxia district and the central district.
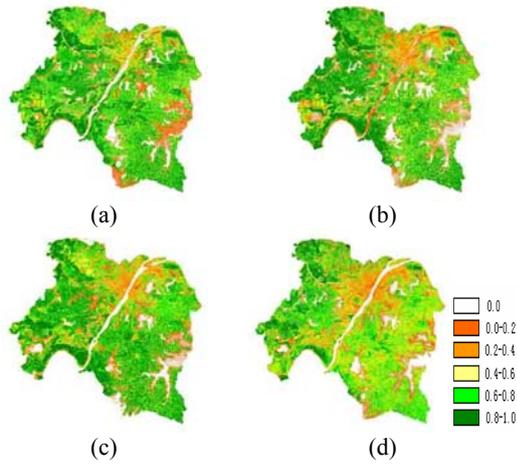

(a)　　　　　　　　(b)

(c)　　　　　　　　(d)

Figure.3 The vegetation fraction in the study area on Oct 26, 1988(a), Oct 23, 1991(b), Oct 4, 1996(c) and Oct 13, 2002(d)

3.3 Relationship between LST and vegetation fraction

Previous studies of relationship between vegetation and temperature[16~18] have proposed a new method ' triangle method', by which the relationships of three parameters, (i.e., vegetation, surface moisture availability and temperature) were discussed. In this study, scatter plots were used to study the relationships between brightness temperature and vegetation fraction. The results are presented in Fig 4, and
the character of the space is nearly triangle. Because when NDVI reached 0.6 or more, where 100 percent vegetation fraction was identified, spatial characteristics of the show were not entirely a triangle.
Fig 2 and Fig 3 show that there was strong negative relationship between LST and vegetation fraction with brightness temperature. It is presented the Vegetation change contributed to the global warming and effected UHI intensity mainly through the processes of urban sprawl, degradation of cropland in this study.
Therefore, we also use the regression analysis to present the relationships quantitatively compared with 'triangle method'. An analysis based on linear regression showed that the coefficient of determination value (R^2) of Wuhan between the above factors was 0.867, 0.843, 0.841, 0.843 of 1988, 1991, 1996 and 2002.

	Vegetation fraction in different time（%）				The change of vegetation fraction in different time（%）		
	1988	1991	1996	2002	1988-1991	1991-1996	1996-2002
caidian	57.36	58.89	58.68	49.99	1.53	-0.21	-8.69
hannan	48.15	52.25	53.37	43.76	4.1	1.12	-9.61
jiangxia	57.71	56.61	59.38	47.73	-1.1	2.77	-11.65
The center urban	50.45	51.76	53.67	43.30	1.31	1.91	-10.37
The whole region	58.41	56.20	57.85	50.45	-2.21	1.65	-7.4

Table. 2　Dynamics of vegetation fraction in different districts of Wuhan in 1988, 1991, 1996 and 2002

4. CONCLUSION

In this paper, qualitative and quantitative analyses have been used to study the change of UHI, vegetation fraction and the relationship between those in Wuhan. Several conclusions were made: (1) distribution of heat island has been expanded rapidly in Wuhan, especially in the center urban; (2) vegetation fraction in Wuhan has decreased through 14 years; (3) the change of vegetation fraction affected UHI intensity, the character of the space between vegetation fraction and temperature is nearly triangle; and there also had a strong negative relationship between vegetation fraction and temperature, the coefficient of determination value (R^2) in different times were larger than 0.8.

The results showed that although remote sensing images were ideal for analyzing UHI and vegetation fraction, it is difficult to select images with similar condition of atmosphere, hydrology.

In future study, several works need to future focused. Firstly, remote sensing images needs to be improved to reduce the influence of thin cloud and inhomogeneous atmosphere condition. Secondly, the impact of the distribution of vegetation fraction in the urbanized area on UHI needs to be further studied.

REFERENCES

Balling, R. C., & Brazell, S. W.. 1988. High resolution surface temperature patterns in a complex urban terrain[J]. *Photogrammetric Engineering and Remote Sensing*, 54 ,pp.1289– 1293

Carlson T N, Capehart W J,Gillies R R., 1995. A new look at the simplified method for remote sensing of daily evapotranspiration[J]. *Remote Sensing of Environment*,54,pp.161~167

Chen Jin, Chen Yunhao, He Chunyang, et al.,2001. Sub-pixel Model for Vegetation Fraction Estimation based on Land Cover Classif ication [J]. *Journal of Remote Sensing*, 5(6) ,pp.416-423.

Chen, Yunhao,Wang, Jie, & Li, Xiaobin.,2002. A study on urban thermal field in summer based on satellite remote sensing[J]. *Remote Sensing for Land and Resources*, 4,pp.55−59

Gallo, K. P., & Owen, T. W. ,1998. Assessment of urban heat island: A multi-sensor perspective for the Dallas-Ft[J]. Worth, USA region. *Geocarto International*, 13,pp.35– 41.

Gallo, K. P., & Owen, T. W.. 1998a. Assessment of urban heat island: A multisensor perspective for the Dallas-Ft. Worth, USA region[J]. *Geocarto International,* 13,pp.35−41.

Gallo, K. P., & Owen, T. W.. 1998b. Satellite-based adjustments for the urban heat island temperature bias[J]. *Journal of Applied Meteorology*, 38, pp. 806−813.

Gallo, K. P., McNab, A. L., Karl, T. R., Brown, J. F., Hood, J. J., & Tarpley, J. D. , 1993. The use of NOAA AVHRR data for assessment of the urban heat island effect[J]. *Journal of Applied Meteorology*, 32,pp.899– 908.

Gillies R R,Carlson T N., 1995. Thermal remote sensing of surface soil water content with partial vegetation cover for incorporation into climate models[J].*Journal of Applied Meteorology*,34,pp.745~756

Kidder, S. Q., & Wu, H. T., 1987. A multispectral study of the St. Louis area under snow-covered conditions using NOAA-7 AVHRR data[J]. *Remote Sensing of Environment*, 22,pp.159–172

Leprieur C, Verstraete M M, Pinty B. , 1994. Evaluation of the Performance of Various Vegetation Indices to Retrieve Vegetation Cover from AVHRR Data [J]. *Remote Sensing Review*, (10) ,pp.265-284.

Lijuan Han, Pengxin Wang, Jindi Wang, et al., 2005. Research on the Characteristic of Space of Vegetation Index-Surface Temperature[J]. *Science of China*,35(4),pp.371~377

Price J C., 1990. Using spatial context in satellite data to infer regional scale evapotranspiration[J].*IEEE Transactions on Geoscience and Remote Sensing*,28,pp.940~948

Roth, M., Oke, T. R., & Emery, W. J., 1989. Satellite derived urban heat islands from three coastal cities and the utilisation of such data in urban climatology[J]. *International Journal of Remote Sensing*, 10,pp.1699~ 1720

Streutker, D. R., 2002. A remote sensing study of the urban heat island of Houston, Texas[J]. *International Journal of Remote Sensing*, 23,pp.2595– 2608

Weng, Q., 2001. A remote sensing-GIS evaluation of urban expansion and its impact on surface temperature in Zhujiang Delta, China[J]. *International Journal of Remote Sensing*, 22(10) ,pp.1999−2014.

Weng, Q., Lu, Dengsheng, & Jacquelyn., 2003. Schubring Estimation of land surface temperature–vegetation abundance relationship for urban heat island studies[J]. *Remote Sensing of Environment*, 89,pp.467−483

Zribi M, Le Hégarat-Mascle, et al., 2003. Derivation of Wild Vegetation Cover Density in Semi-arid Region: ERS2/SAR Evaluation [J]. *International Journal of Remote Sensing*, (24) ,pp.1335-1352.